This article was downloaded by:
On: *25 January 2011*
Access details: *Access Details: Free Access*
Publisher *Taylor & Francis*
Informa Ltd Registered in England and Wales Registered Number: 1072954 Registered office: Mortimer House, 37-41 Mortimer Street, London W1T 3JH, UK

Separation Science and Technology
Publication details, including instructions for authors and subscription information:
http://www.informaworld.com/smpp/title~content=t713708471

Binary Adsorption in a Fixed-Bed Column Packed with an Ion-Exchange Resin

Run-Tun Huang[a]; Teh-Liang Chen[a]; Hung-Shan Weng[a]
[a] DEPARTMENT OF CHEMICAL ENGINEERING, NATIONAL CHENG KUNG UNIVERSITY, TAINAN, TAIWAN

To cite this Article Huang, Run-Tun , Chen, Teh-Liang and Weng, Hung-Shan(1995) 'Binary Adsorption in a Fixed-Bed Column Packed with an Ion-Exchange Resin', Separation Science and Technology, 30: 13, 2731 — 2746
To link to this Article: DOI: 10.1080/01496399508013712
URL: http://dx.doi.org/10.1080/01496399508013712

PLEASE SCROLL DOWN FOR ARTICLE

Full terms and conditions of use: http://www.informaworld.com/terms-and-conditions-of-access.pdf

This article may be used for research, teaching and private study purposes. Any substantial or systematic reproduction, re-distribution, re-selling, loan or sub-licensing, systematic supply or distribution in any form to anyone is expressly forbidden.

The publisher does not give any warranty express or implied or make any representation that the contents will be complete or accurate or up to date. The accuracy of any instructions, formulae and drug doses should be independently verified with primary sources. The publisher shall not be liable for any loss, actions, claims, proceedings, demand or costs or damages whatsoever or howsoever caused arising directly or indirectly in connection with or arising out of the use of this material.

SEPARATION SCIENCE AND TECHNOLOGY, **30**(13), pp. 2731–2746, 1995

Binary Adsorption in a Fixed-Bed Column Packed with an Ion-Exchange Resin

RUN-TUN HUANG, TEH-LIANG CHEN,
and HUNG-SHAN WENG*
DEPARTMENT OF CHEMICAL ENGINEERING
NATIONAL CHENG KUNG UNIVERSITY
TAINAN, TAIWAN 70101, REPUBLIC OF CHINA

Downloaded At: 11:59 25 January 2011

ABSTRACT

A mathematical model was adopted to analyze a binary fixed-bed adsorption column packed with an ion-exchange resin. Two pairs of organic compounds, *o*-cresol–benzoic acid and *p*-chlorophenol–*p*-nitrophenol, were employed as the adsorbates. A modified Langmuir isotherm with interaction factors η_i was found suitable for representing the adsorption equilibrium. Scale-up of the binary adsorption column with respect to column length was effective based on the proposed mathematical model and corresponding methods for estimating the model parameters. The significance of excess concentration in the breakthrough curve was related to inlet concentration, column length, and the difference in adsorption affinity.

Key Words. Binary adsorption column; Langmuir isotherm; Solid-diffusion model

INTRODUCTION

Fixed-bed adsorption has found considerable application in the separation and purification of liquid mixtures. Examples include water treatment and recovery of biological products. Early reports on this subject have focused on single-component systems. In practice, however, the feed

* To whom correspondence should be addressed.

Copyright © 1995 by Marcel Dekker, Inc.

stream to a fixed-bed adsorption column often contains a broad range of adsorbates, and between the adsorbates there exist interactions. This fact complicates the theoretical description for a multicomponent adsorption column.

Although multicomponent adsorption systems have recently received increasing attention, in the literature there still exists little information on column performance. Successful simulation of a fixed-bed adsorption column depends mainly on the choice of an adequate mathematical model. To develop a mathematical model that describes the adsorption process, four equations are essential: mobile phase mass balance, external film diffusion, intraparticle diffusion, and adsorption kinetics. Among these four relations, adsorption kinetics represents the major difference between single- and multicomponent adsorptions.

In general, the adsorption rate is much faster than the diffusion rate, so that equilibrium can be assumed at every local position. The most simple equilibrium model of a single component that has been used is the Langmuir isotherm:

$$\frac{q}{q_m} = \frac{aC_s}{1 + aC_s} \tag{1}$$

With the further assumption of identical saturation capacities for all components, the single-component Langmuir isotherm, Eq. (1), has been extended to multicomponent adsorptions (1):

$$\frac{q_i}{q_{mi}} = \frac{a_i C_{si}}{1 + \sum_{i=1}^{n} a_i C_{si}} \tag{2}$$

where the a_i's are derived from the corresponding individual Langmuir isotherm equations. However, it is unrealistic to assume identical saturation capacities for different solutes. Besides, multicomponent adsorptions are complicated by interactive and/or competitive effects of the solutes. Accordingly, prediction of mixture isotherms solely from isotherm data of the single solutes is impractical. To make improvement to Eq. (2), Schay et al. (2) proposed a modified model with interaction factors η_i extracted from experimental competitive isotherms:

$$\frac{q_i}{q_{mi}} = \frac{a_i C_{si}/\eta_i}{1 + \sum_{i=1}^{n} a_i C_{si}/\eta_i} \tag{3}$$

Intraparticle diffusion is an important mass transfer step in an adsorption process. Both solid- and pore-diffusion models have been widely used

Downloaded At: 11:59 25 January 2011

to describe diffusion in a porous adsorbent (3). In a previous study on a single-component adsorption column (4), the solid-diffusion model was found to be more suitable for modeling favorable adsorptions onto an ion-exchange resin than the pore-diffusion model.

The aim of this study was to examine the suitability of a combination of the modified Langmuir model (Eq. 3) and the solid-diffusion model for analyzing binary fixed-bed adsorption columns. An anion-exchange resin was used as the adsorbent. Two pairs of organic compounds, *o*-cresol–benzoic acid and *p*-chlorophenol–*p*-nitrophenol, were employed as the adsorbates. Scale-up experiments of the binary adsorptions with respect to column length were carried out to evaluate the proposed mathematical model. In addition, the relationships of excess concentration in the breakthrough curve with adsorption affinity, inlet concentration, and column length are discussed.

MATHEMATICAL MODELS

Downloaded At: 11:59 25 January 2011

The fixed-bed adsorption column is assumed to be packed with spherical particles of radius R. The mass transfer processes include axial dispersion, intraparticle diffusion, and external film diffusion. The diffusional process within the adsorbents is described by the solid-diffusion model. Local equilibrium between the solid phase and the fluid phase is assumed with the modified Langmuir isotherm, Eq. (3). The breakthrough curve of component i can thus be obtained from the following set of equations.

Mobile phase mass balance:

$$\frac{\partial C_i}{\partial t} + v\frac{\partial C_i}{\partial z} - D_L\frac{\partial^2 C_i}{\partial z^2} = -\frac{1-\epsilon_b}{\epsilon_b}\rho D_{si}\left(\frac{3}{R}\right)\left.\frac{\partial q_i}{\partial r}\right|_{r=R} \tag{4}$$

Particle diffusion:

$$\frac{\partial q_i}{\partial t} = D_{si}\left(\frac{\partial^2 q_i}{\partial r^2} + \frac{2}{r}\frac{\partial q_i}{\partial r}\right) \tag{5}$$

External film diffusion:

$$\rho D_{si}\frac{\partial q_i}{\partial r} = k_{fi}(C_i - C_{si}), \qquad \text{at } r = R \tag{6}$$

Adsorption isotherm:

$$\frac{q_i}{q_{mi}} = \frac{a_i C_{si}/\eta_i}{1 + a_1 C_{s1}/\eta_1 + a_2 C_{s2}/\eta_2} \tag{7}$$

Initial conditions:

$$C_i = 0, \quad \text{at } t = 0 \tag{8}$$

$$q_i = 0, \quad \text{at } t = 0 \tag{9}$$

Boundary conditions:

$$C_i = C_{0i}, \quad \text{at } z = 0 \tag{10}$$

$$\partial C_i/\partial z = 0, \quad \text{at } z = L \tag{11}$$

$$\partial q_i/\partial r = 0, \quad \text{at } r = 0 \tag{12}$$

MATERIALS AND METHODS

Most materials and methods used in this study were the same as those used in the previous work (4). Ion Exchanger II (weak base, Merck, Art No. 4766) of size 28–35 mesh was employed as the adsorbent. The resin was immersed in 1 N NaOH solution for conversion to the OH-form. The average diameter of the swollen resin, measured by a profile projector, was 0.02522 cm. The apparent density of the wet resin was found to be 0.476 g/cm^3, and its true density was 1.116 g/cm^3.

Adsorption equilibrium was obtained according to the following material balance:

$$q = \frac{(C_I - C_e)V}{W} \tag{13}$$

The initial concentration of each solute employed in the equilibrium experiment was 13.0 μmol/cm^3. Various amounts of Ion Exchanger II were used to generate the equilibrium data. Equilibrium was achieved in a shaker after about 6 days at 27°C. The concentration of each solute was determined by a UV spectrophotometer (Hitachi, Model U-2000). The molar absorptivities employed are given in Table 1. The procedure for determining the concentration of a bisolute system has been described elsewhere (5).

Column experiments were carried out in a glass tube of 1.142 cm. The solutions were fed upward in all the experiments. The void fraction in the bed, ϵ_b, was estimated from the volume of water which occupied the intergranular space in the ion-exchange column, according to the following equation (6):

$$\epsilon_b = 1.05 \times \frac{\text{volume of drained water}}{\text{bed volume}} \tag{14}$$

where 1.05 was used to account for the inclusion of incomplete drainage

Downloaded At: 11:59 25 January 2011

TABLE 1
Molar Absorptivities of Organic Compounds at Various Wavelength

Compound	Wavelength (nm)	Absorptivity ($cm^3/mmol \cdot cm$)
o-Cresol	223	2476
	270	1473
Benzoic acid	223	7993
	270	468
p-Chlorophenol	243	826
	280	4140
p-Nitrophenol	243	4599
	280	4980

of water from the bed. The values of the bed void fraction obtained in all experiments were around 0.345.

Axial dispersion is a function of physical factors like flow rate and particle size of the adsorbent, but not of chemical differences between solutes. The axial dispersion coefficient for the liquid flowing through fixed beds was obtained from the correlation equation of Chung and Wen (7):

$$\frac{D_L \rho_L}{\mu} = \frac{\mathrm{Re}}{0.20 + 0.011\mathrm{Re}^{0.48}} \tag{15}$$

Equation (15) is applicable in the Reynolds number range of 10^{-3} to 10^3. The film mass transfer coefficient k_f was calculated from (8, 9)

$$\frac{2Rk_f}{D_m} = 2.0 + 1.45\mathrm{Re}^{1/2}\mathrm{Sc}^{1/3} \tag{16}$$

where the molecular diffusivity, D_m, was estimated from the equation of Wilke and Chang (10).

To obtain the breakthrough curves, the dimensionless forms of Eqs. (4)–(12) were first treated by the orthogonal collocation method. The resulting ordinary differential equations were then solved by the method of DGEAR. Four collocation points for both column length and particle radius were found to be adequate in the calculation. The only unavailable parameter in the mathematical model, intraparticle diffusivity D_s, was determined by fitting the model breakthrough curve to that of the experiment, in which a two-dimensional simplex (11) was employed for the parameter estimation. The optimization criterion chosen was the minimum total square error. All the computations were done on a 486 personal computer.

Downloaded At: 11:59 25 January 2011

RESULTS AND DISCUSSION

Analysis of Equilibrium Data

An accurate representation of single-component adsorption equilibria is a prerequisite for simulating multicomponent adsorptions. Figure 1 gives the equilibria data for two pairs of adsorbates: *o*-cresol–benzoic acid and *p*-chlorophenol–*p*-nitrophenol. *o*-Cresol shows an approximately linear adsorption isotherm; benzoic acid exhibits a very favorable one; and the shapes of isotherms for *p*-chlorophenol and *p*-nitrophenol are favorable. It should be pointed out that the difference in adsorption affinities between the former pair is large, while it is small between the latter pair. Analyzing the equilibria data with the single-component Langmuir isotherm, Eq. (1), a and q_m were obtained as given in Table 2.

In Fig. 2 is shown the experimental and theoretical bisolute equilibrium data for *o*-cresol and benzoic acid. Obviously, application of the extended Langmuir isotherm, Eq. (2), which does not consider the interactive and/or competitive effects of the solutes, is not in agreement with the experimentals. In other words, the bisolute isotherm of *o*-cresol–benzoic acid cannot be predicted solely from the single-component ones.

Compared with benzoic acid, *o*-cresol is a weak adsorbate. As a result, it cannot be adsorbed as much as Eq. (2) predicted due to the competitive

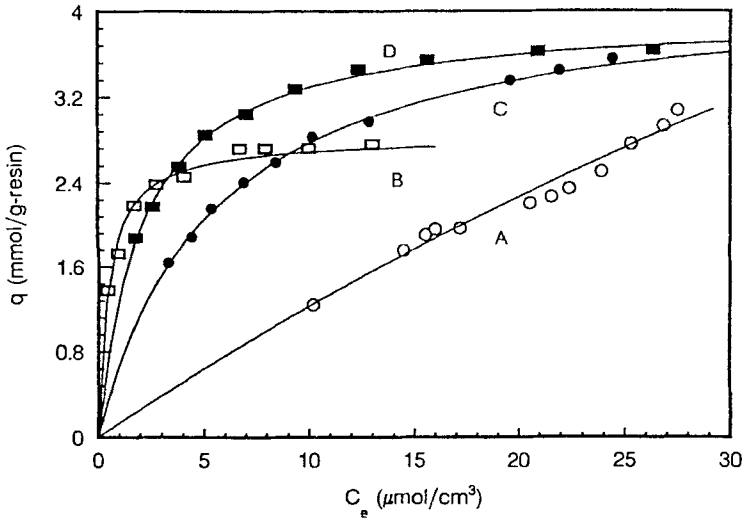

FIG. 1 Single-component equilibrium isotherm: (A) *o*-cresol, (B) benzoic acid, (C) *p*-chlorophenol, (D) *p*-nitrophenol.

Downloaded At: 11:59 25 January 2011

TABLE 2
Estimated Constants of Langmuir Isotherms

Compound	a (cm^3/μmol)	q_m (mmol/g-resin)	η
o-Cresol	0.01124	12.223	1.260
Benzoic acid	1.906	2.849	0.842
p-Chlorophenol	0.184	4.270	1.084
p-Nitrophenol	0.487	3.965	0.976

effect between the solutes. It is therefore supposed that the extended Langmuir isotherm overestimates the adsorption of the weaker adsorbate. A similar phenomenon also occurs in the case of *p*-chlorophenol–*p*-nitrophenol, as shown in Fig. 3. The extents of this overestimation for the weaker adsorbates are closely related to the relative values of the adsorption affinities of the competing solutes. From Figs. 2 and 3 it can be seen that the extent of overestimation for *o*-cresol is more significant than for

Downloaded At: 11:59 25 January 2011

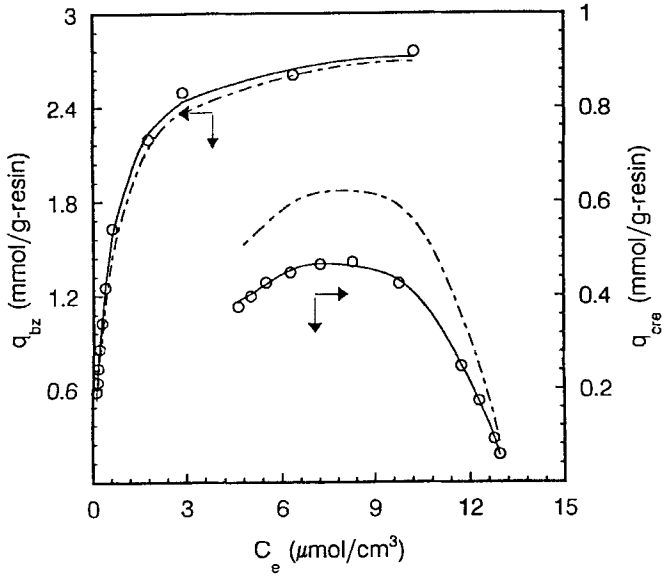

FIG. 2 Experimental and theoretical bisolute equilibria data for *o*-cresol and benzoic acid. (○) Experimental data; (– -) extended Langmuir isotherm, Eq. (2); (——) modified Langmuir isotherm, Eq. (3).

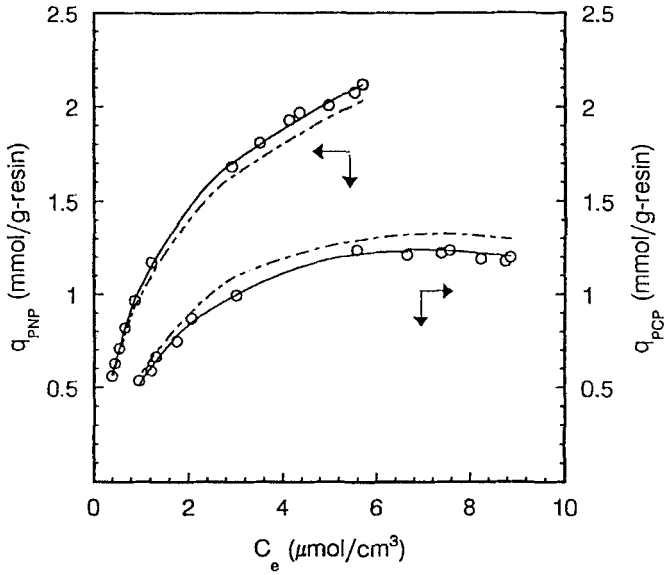

FIG. 3 Experimental and theoretical bisolute equilibria data for *p*-chlorophenol and *p*-nitrophenol. (O) Experimental data; (– -) extended Langmuir isotherm, Eq. (2); (——) modified Langmuir isotherm, Eq. (3).

Downloaded At: 11:59 25 January 2011

p-chlorophenol. It is therefore implied that the larger difference in the adsorption affinity, the larger deviation of the solid-phase concentration of the weaker adsorbate from the predicted value.

Benzoic acid and *p*-nitrophenol, on the other hand, are the stronger adsorbates in each pair, and thus are favored in the competition for adsorption. Accordingly, underestimations for benzoic acid and *p*-nitrophenol in the solid-phase concentration are expected. Nevertheless, deviation from the predicted value from Eq. (2) is less significant for the stronger adsorbates because they are dominating species.

By adopting the interaction factor η, the modified Langmuir isotherm, Eq. (3), can well represent the experimental data (as shown in Figs. 2 and 3). The values of η_i obtained by curve fitting are given in Table 2.

Fittings of the Breakthrough Data

The experimental binary breakthrough data for *o*-cresol and benzoic acid on columns of 10, 20, and 30 cm length are shown in Fig. 4. The feed

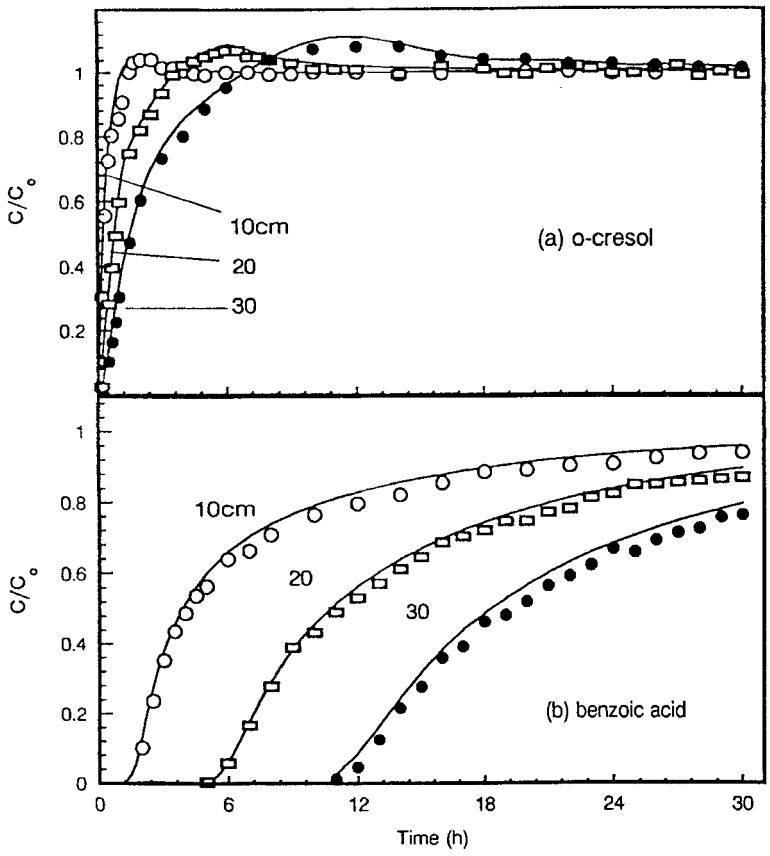

FIG. 4 Breakthrough curves for *o*-cresol and benzoic acid on columns of 10, 20, and 30 cm length. Symbols, experimental; lines, calculated. C_0 = 4.87 μmol/cm³ for both solutes, Q = 6.16 cm³/min.

rate introduced to the column was 6.16 cm³/min. Both solutes were at concentrations of 4.87 μmol/cm³. The mass transfer parameters estimated for the calculation of breakthrough curves were D_L = 1.44 cm²/min, $k_{f,cre}$ = 0.1464 cm/min, and $k_{f,bz}$ = 0.1442 cm/min. Fitting the mathematical model, Eqs. (4)–(12), to the 10-cm experimental breakthrough data, the surface diffusivity D_{si} were estimated as 8.51×10^{-8} and 8.03×10^{-8} cm²/min for *o*-cresol and benzoic acid, respectively. The agreement of the calculated breakthrough curves to that of experiment is quite good.

Downloaded At: 11:59 25 January 2011

According to the solid-diffusion model, the solute is adsorbed on the outer surface of the adsorbents, followed by the diffusion of the adsorbate in the adsorbed state. Benzoic acid is more strongly bonded to the adsorbent than *o*-cresol. Consequently, the solid diffusion of benzoic acid molecules in the adsorbent particle is slower than *o*-cresol molecules, and a smaller value of D_s for benzoic acid than for *o*-cresol was expected.

Prediction of Breakthrough Curves for Longer Columns

The estimated D_{si}'s were then used to predict breakthrough curves for longer adsorption beds. As one can see from Fig. 4, the experimental data for column lengths of 20 and 30 cm coincide well with the predictions based on the mathematical model. The close agreement between the experimental data and the calculated curves indicates that the proposed mathematical model and methods for determining corresponding parameters can perform effectively for the binary adsorption column.

Downloaded At: 11:59 25 January 2011

Characteristics of Excess Concentration

In Fig. 4(a) it is noted that a peak of excess concentration appears in each of the breakthrough curves of *o*-cresol, which is a common phenomenon in multicomponent adsorption columns and is caused by a displacement effect (12–16). Due to the difference in the adsorption affinity, a chromatographic separation of *o*-cresol and benzoic acid occurs within the column. At the beginning of the column performance, benzoic acid, being the stronger adsorbate, is adsorbed near the influent end of the column while *o*-cresol (the weaker adsorbate) is largely adsorbed further along the bed. As the feeding continues, benzoic acid moves as a wave front down the bed, which results in a competitive binary sorption regime. Consequently, some previously adsorbed *o*-cresol is displaced by benzoic acid. An enrichment of *o*-cresol in the liquid phase thus results.

The significance of the excess concentration in the breakthrough curve of the weaker adsorbate is related to inlet concentration. From Fig. 5 one can see that the peak height decreases with decreasing inlet concentrations of both *o*-cresol and benzoic acid. As described above, the excess concentration is a result of displacement effect. For this phenomenon to occur, apparently there should exist sufficient amounts of *o*-cresol and/or benzoic acid. Nevertheless, it is interesting to find out what species is determinant in the concentration-dependency. Keeping the concentration of *o*-cresol constant, the peak height was found to decrease with decreasing concentration of benzoic acid, as shown in Fig. 6. The variation in the breakthrough curves is very close to that in Fig. 5. On the contrary, as

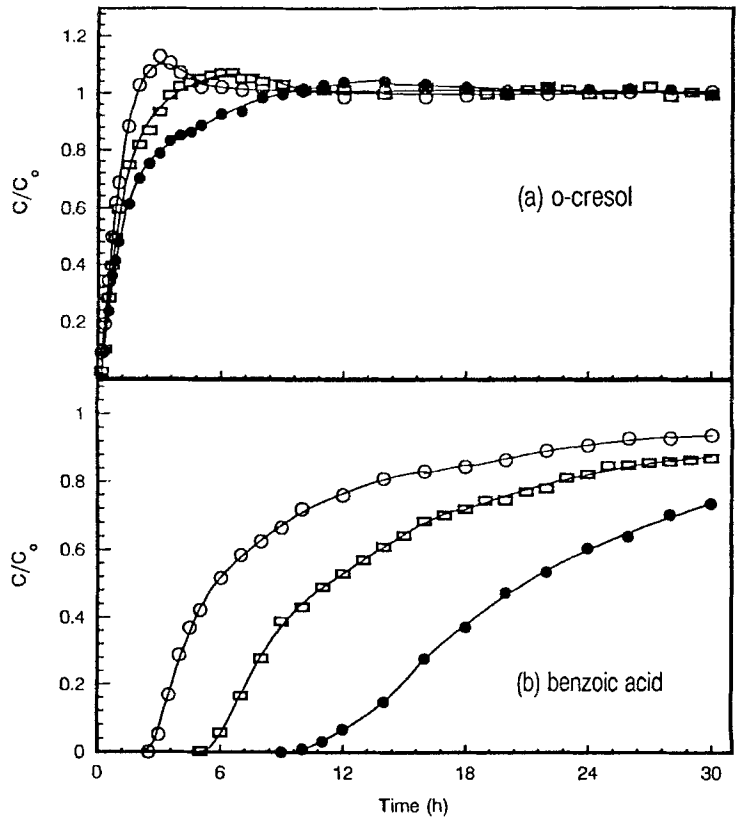

FIG. 5 Experimental breakthrough curves for *o*-cresol and benzoic acid at various inlet concentrations. C_0: (○) 8.64, (□) 4.87, and (•) 2.44 μmol/cm³. L = 20 cm, Q = 6.16 cm³/min.

depicted in Fig. 7, if the concentration of *o*-cresol was decreased while keeping the concentration of benzoic acid constant, the peak height was not significantly changed. It is therefore concluded that the significance of the excess concentration depends mainly on the concentration of the stronger adsorbate rather than the weaker adsorbate.

The peak height of the excess concentration in the breakthrough curve of the weaker adsorbate is also related to column length. The weaker adsorbate must be adsorbed onto the adsorbent prior to the displacement by the stronger adsorbate. Therefore, if we shorten the column length to

Downloaded At: 11:59 25 January 2011

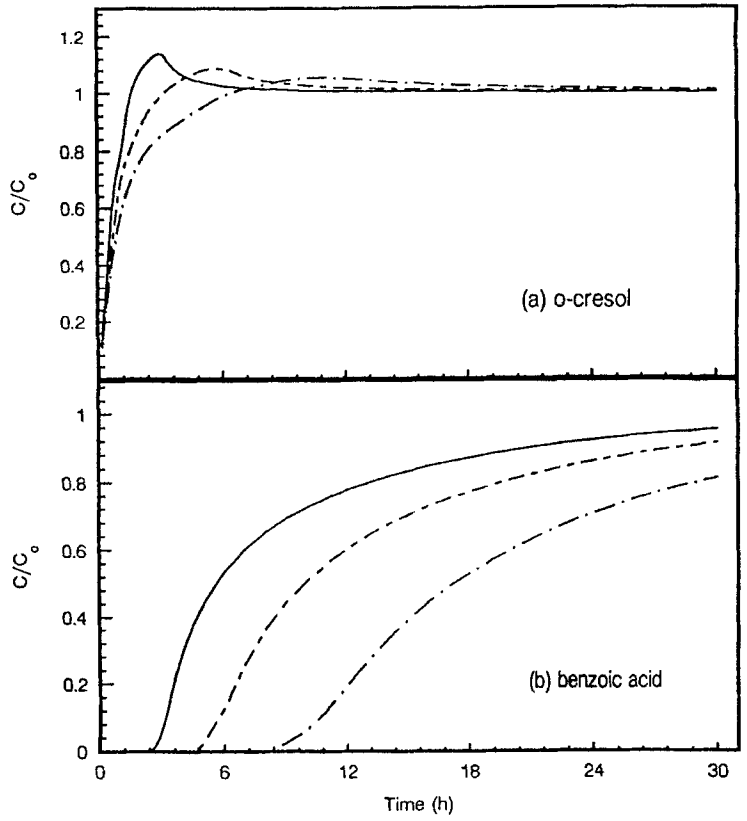

FIG. 6 Variation of the excess peak composition with the concentration of benzoic acid at an *o*-cresol concentration of 8.64 μmol/cm^3. $C_{o,bz}$: (——) 8.64, (– -) 4.87, and (–·–) 2.44 μmol/cm^3.

an extreme, it can be said that there is negligible adsorption of the weaker adsorbate on the bed, and the displacement effect will not be observed. If the column is lengthened, on the other hand, the amount of the weaker adsorbate available for displacement will increase. Accordingly, the extent of enrichment of the weaker adsorbate in the liquid phase is increased, and a more remarkable excess concentration can be observed. This trend can be found in Fig. 4(a). For compounds with similar adsorption affinities (say, *p*-chlorophenol and *p*-nitrophenol), the displacement effect is not

Downloaded At: 11:59 25 January 2011

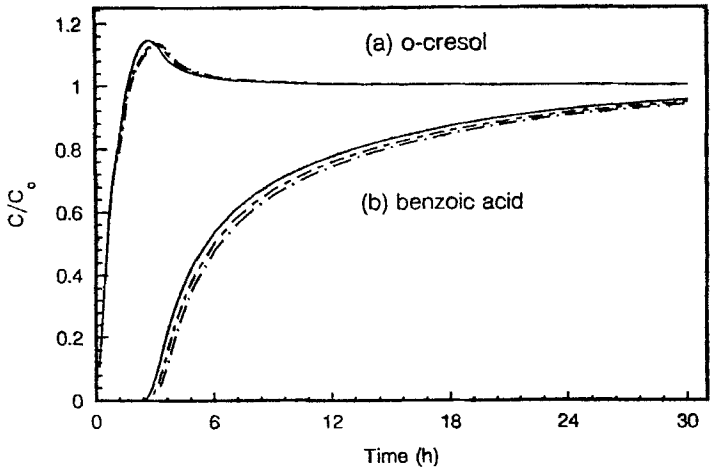

FIG. 7 Variation of the excess peak composition with the concentration of *o*-cresol at a benzoic acid concentration of 8.64 μmol/cm³. $C_{0,cre}$: (——) 8.64, (– -) 4.87, and (–·–) 2.44 μmol/cm³.

Downloaded At: 11:59 25 January 2011

apparent, and excess concentrations can only be observed in long columns, as shown in Fig. 8.

From Fig. 4 we noted that the timings of the appearance of the peak of excess concentration of *o*-cresol and the breakthrough point of benzoic acid were about the same. This is a clear indication of a strong displacement effect, which primarily arises from a large difference in the adsorption affinities of the two solutes. As an extreme case of a binary adsorption column with two solutes of equal adsorption affinities, the breakthrough points are the same and excess concentration will never occur. Based on this reasoning, for cases with small differences in adsorption affinity, the displacement effect will not be remarkable and the breakthrough point of the stronger adsorbate will appear prior to the peak of excess concentration of the weaker adsorbate. Therefore, it can be said that the smaller this time period, the larger will be the difference in the adsorption affinity. An illustration of such a situation can be found in Fig. 8. The time period between the breakthrough point of the stronger adsorbate and the peak of excess concentration of the weaker adsorbate could therefore be a qualitative or even a quantitative representation of the difference of adsorption affinities.

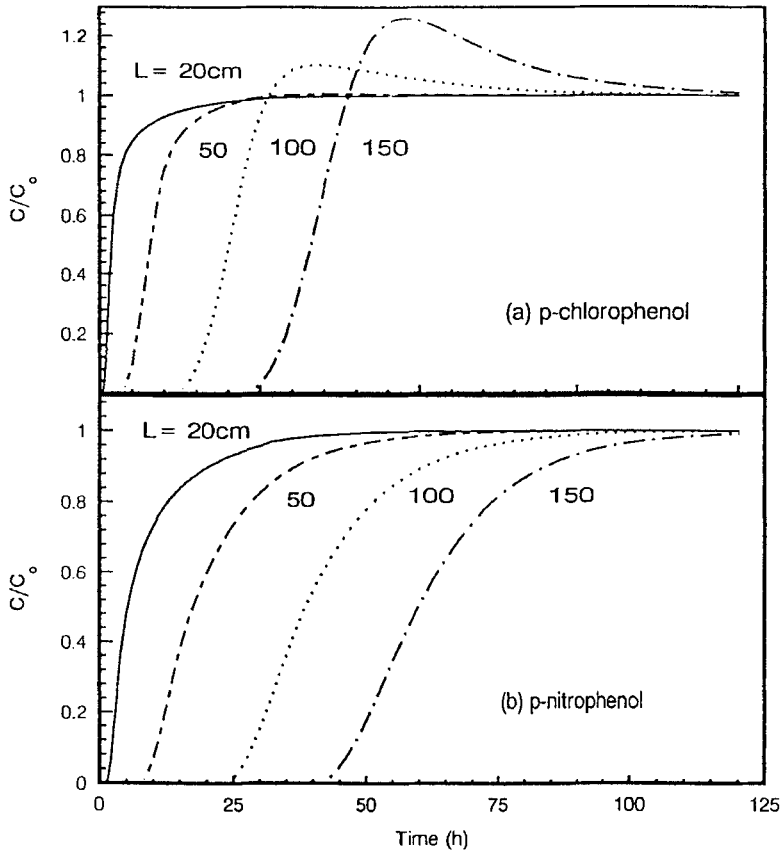

FIG. 8 Breakthrough curves for *p*-chlorophenol and *p*-nitrophenol on different column lengths. $C_{0,pcp}$ = 9.25 μmol/cm³, $C_{0,pnp}$ = 9.32 μmol/cm³, Q = 10.2 cm³/min, D_L = 2.36 cm²/min, $k_{f,pcp}$ = 0.1831 cm/min, and $k_{f,pnp}$ = 0.1785 cm/min. 20-cm curve: fitting of experimental data. 50-, 100-, and 150-cm curves: calculated.

CONCLUSIONS

Binary adsorptions of *o*-cresol–benzoic acid and *p*-chlorophenol–*p*-nitrophenol onto Ion Exchanger II can be well represented by the modified Langmuir isotherm with interaction factors η_i extracted from experimental competitive isotherms. Simulation of fixed-bed column adsorption for binary systems is effective with a solid-diffusion model previously used in

Downloaded At: 11:59 25 January 2011

single-component adsorption (4). The occurrence of excess concentration in the breakthrough curve is caused by the displacement effect between solutes. As the inlet concentrations, the column length, or the difference in adsorption affinity increases, the excess concentration becomes more apparent. In the concentration-dependency, the excess concentration is mainly related to the concentration of the stronger adsorbate rather than the weaker adsorbate.

ACKNOWLEDGMENT

This study was supported by Research Grant NSC83-0402-E006-009, National Science Council of the Republic of China.

NOMENCLATURE

a	Langmuir constant (cm^3/mol)
C	solute concentration in mobile phase (mol/cm^3)
C_e	solute concentration in liquid phase at equilibrium (mol/cm^3)
C_I	initial solute concentration used in the equilibrium experiment (mol/cm^3)
C_s	equilibrium liquid-phase concentration (mol/cm^3)
C_0	inlet concentration of solute (mol/cm^3)
D_L	axial dispersion coefficient (cm^2/min)
D_m	molecular diffusivity (cm^2/min)
D_s	surface diffusivity (cm^2/min)
k_f	film mass transfer coefficient (cm/min)
L	bed length (cm)
Q	volumetric flow rate of feed stream (cm^3/min)
q	solute concentration in solid phase (mol/g-resin)
q_m	maximum solid phase concentration of solute (mol/g-resin)
q_0	solid phase concentration of solute in equilibrium with C_0 (mol/g-resin)
R	particle radius (cm)
r	radial distance from center of spherical particle (cm)
Re	Reynolds number ($2Ru_0\rho_L/\mu$) (dimensionless)
Sc	Schmidt number ($\mu/\rho_L D_m$) (dimensionless)
t	time (minutes)
u_0	superficial velocity (cm/min)
V	liquid volume (cm^3)
v	interstitial fluid velocity (cm/min)

Downloaded At: 11:59 25 January 2011

W weight of resin (g)
z distance in flow direction (cm)

Greek Letters

ϵ_b bed void fraction (dimensionless)
η interaction factor (dimensionless)
μ liquid viscosity (g/cm·min)
ρ density of the adsorbent particle (g-resin/cm^3)
ρ_L density of liquid (g/cm^3)

Subscripts

bz benzoic acid
cre *o*-cresol
i *i*th component
pcp *p*-chlorophenol
pnp *p*-nitrophenol

Downloaded At: 11:59 25 January 2011

REFERENCES

1. J. A. V. Butler and C. J. Ockrent, *J. Phys. Chem.*, *34*, 2841 (1930).
2. G. J. Schay, F. P. Fejes, and J. Szethmary, *Acta Chim. Acad. Sci. Hung.*, *12*, 299 (1957).
3. T. W. Weber and R. K. Chakravorti, *AIChE J.*, *20*, 228 (1974).
4. R. T. Huang, T. L. Chen, and H. S. Weng, *Sep. Sci. Technol.*, *29*, 2019 (1994).
5. D. A. Skoog, *Principles of Instrumental Analysis*, 3rd ed., Saunders College Publishing, Philadelphia, 1985, p. 213.
6. Mitsubishi Chemical Industries Limited, *Diaion: Manual of Ion Exchange Resins* (*1*), revised ed., Tokyo, Japan, 1980, p. 89.
7. S. F. Chung and C. Y. Wen, *AIChE J.*, *14*, 857 (1968).
8. N. Wakao, T. Oshima, and S. Yagi, *Chem. Eng. Jpn.*, *22*, 780 (1958).
9. S. C. Foo and R. G. Rice, *AIChE J.*, *21*, 1149 (1975).
10. C. R. Wilke and P. Chang, *Ibid.*, *1*, 264 (1955).
11. G. S. G. Beveridge and R. S. Schechter, *Optimization: Theory and Practice*, McGraw-Hill, New York, 1970, p. 367.
12. R. L. Gariepy and I. Zwiebel, *AIChE Symp. Ser.*, *67*(117), 17 (1971).
13. T. M. Keinath, *Ibid.*, *73*(166), 1 (1976).
14. J. S. C. Hsieh, R. M. Turian, and C. Tien, *AIChE J.*, *23*, 263 (1977).
15. A. I. Liapis and D. W. T. Rippin, *Chem. Eng. Sci.*, *33*, 593 (1978).
16. W. Merk, W. Fritz, and E. U. Schlunder, *Ibid.*, *36*, 743 (1980).

Received by editor October 24, 1994